J|A|C|S COMMUNICATIONS

Published on Web 04/14/2010

Intracellular Bioconjugation of Targeted Proteins with Semiconductor Quantum Dots

Kelly Boeneman,[†] James B. Delehanty,[†] Kimihiro Susumu,[‡] Michael H. Stewart,[‡] and Igor L. Medintz*,[†]

Center for Bio/Molecular Science and Engineering, Code 6900, Optical Sciences Division, Code 5611, U.S. Naval Research Laboratory, 4555 Overlook Avenue, S.W., Washington, D.C. 20375

Received January 9, 2010; E-mail: Igor.Medintz@nrl.navy.mil

One of the most basic experimental formats in biological research continues to be the selective fluorescent labeling of intracellular proteins for monitoring and understanding their spacio-temporal activity. Recombinant strategies to accomplish this commonly fuse fluorescent proteins directly to the target of interest[1] or engineer chimeric enzyme-target fusions that bind exogenously added fluorescent substrates.[2] Examples of the latter include the mutated haloalkane dehalogenase enzyme (HaloTag) which irreversibly binds a halogenated alkane-modified substrate,[2a] expressed protein ligation with split inteins,[2b] and acyl carrier proteins systems.[2c] Chemical or affinity interactions specifically targeting small peptidyl handles appended onto proteins are also available as exemplified by Tsien's FlAsH/ReAsH biarsenical fluorophores[3a] which react with vicinal tetracysteine motifs and nitrilotriacetic acid (NTA) functionalized dye coordination to oligohistidine (His_n) sequences.[3b] His_n motifs were originally appended to proteins to allow their purification over Ni^{2+}-NTA media.[3c] Although these chemistries all facilitate *in vivo* labeling of target proteins, they are still limited by the intrinsic photophysical properties of the fluorophores themselves. For example, fluorescent proteins have long maturation times and organic dyes commonly suffer from low quantum yields (QYs) and ionic/pH sensitivity.[4] Both fluorophore species are also highly susceptible to photobleaching. Taken together, these issues can significantly complicate long-term *in vivo* monitoring of labeled proteins.

In contrast, the optical properties of semiconductor quantum dots (QDs) suggest they are ideally suited for long-term monitoring of intracellular protein dynamics. These include high QYs, resistance to chemical degradation, photostability, large "effective" Stokes shifts, and choice of size-tunable, narrow-symmetric photoluminescence (PL) ranging from the UV to near-IR.[4a,5] These properties also make them useful for multiplexing applications as well as single-molecule tracking and allow them to function as unique Förster resonance energy transfer (FRET) donors.[4a,5] Impediments to further QD-cellular application arise from two issues: (1) limited chemistries to attach desired biomolecules onto the QDs with control over valence (ratio), orientation, and binding affinity; (2) limited methods to deliver the QD-bioconjugates into the cytoplasm of live cells.[6] Commonly used peptide and polymer-based cellular delivery methods (cell penetrating peptides or transfection agents, respectively) almost always result in conjugate sequestration within the endolysosomal system.[6] Clearly, the ability to uniquely conjugate QDs to a target protein *in vivo* is highly desirable, and expanding the intracellular fluorescent labeling "toolset" to include these unique nanomaterials will provide far more versatile research formats. Here we demonstrate a strategy allowing specific cytoplasmic proteins to be conjugated to QDs intracellularly and utilize FRET to both characterize and confirm this process *in vivo*.

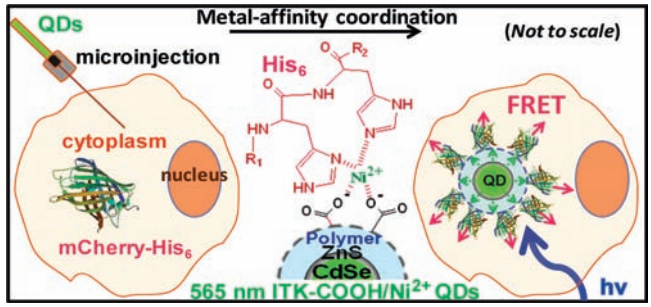

Figure 1. Protein-His_n/QD intracellular assembly. Cells expressing mCherry-His_6 proteins are microinjected with Ni^{2+}-supplemented 565 nm ITK-COOH QDs (left) resulting in His_6-driven protein coordination to the Ni^{2+}-COOH QD surfaces (right). Putative interactions of His residues with QD-chelated Ni^{2+} are shown in the center. QD excitation results in FRET-sensitized emission from mCherry confirming the intracellular assembly.

We have previously reported the use of metal-affinity coordination between His_n residues and the ZnS shell of CdSe/ZnS QDs as a method for conjugating proteins, peptides, and even modified DNA sequences to the nanocrystals to create a variety of FRET-based sensors.[6−9] QD-His_n interactions are characterized by strong binding affinities (K_d^{-1} $\sim 1 \times 10^9$ M^{-1}), which are stable in cellular environments and allow for control over valence and biomolecular orientation on the QDs in most cases.[7] Bawendi exploited this conjugation to link His_6-streptavidin to QDs for subsequent labeling of extracellular membrane receptors bound to biotinylated ligands,[7c] and in an elegant demonstration, Dahan combined this chemistry with selective biotinylation of acceptor peptides to realize two-color single QD tracking of extracellular membrane proteins.[7d] This same bioconjugation can also be applied to commercial polymer-functionalized QDs. Dennis showed that EviTag QDs (Evident Technologies) capped with a lipid/polyethylene glycol-(PEG) ligand still allowed metal-affinity binding of His_6-tagged fluorescent proteins to the QD surface.[7e] Analysis of FRET between the QD donor and the conjugated protein acceptors confirmed their close proximity. Rao's group demonstrated that Invitrogen QDs capped with a carboxylated polymer could also coordinate His_6-tagged luciferase enzymes to create protease sensors that transduced a signal via bioluminescence resonance energy transfer (BRET).[7f] Adding excess Ni^{2+} to the QDs significantly increased His_6-luciferase binding and BRET interactions, suggesting QD-surface carboxyl groups chelated Ni^{2+} and bound protein in a manner similar to that of NTA groups. Given these facts, we reasoned that an appropriate fluorescent protein-His_n/QD combination could assemble *intracellularly* and FRET monitoring should allow *in vivo* confirmation of this interaction; see Figure 1.

Recently, we described the FRET interactions between 550 nm emitting QD donors solubilized with dihydrolipoic acid (DHLA) and His_6-appended mCherry acceptors self-assembled on their surfaces along with their use

[†] Center for Bio/Molecular Science and Engineering.
[‡] Optical Sciences Division.

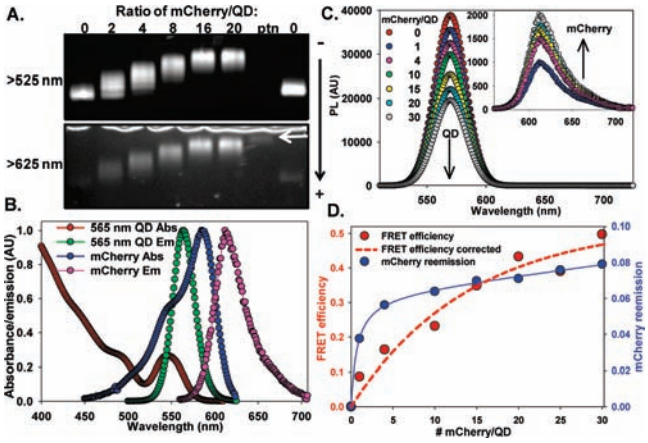

Figure 2. (A) 565 nm ITK carboxyl/Ni^{2+} QDs assembled with increasing mCherry-His_6 separated in 1% agarose gels and visualized with >525 nm (QD and mCherry PL) and >625 nm (mCherry PL only) long-pass filters. Arrow indicates 20 mCherry without QD. (B) Normalized absorption and PL spectra of 565 nm QD-mCherry pair; QD-quantum yield 69%, mCherry extinction coefficient 71 000 M^{-1} cm^{-1} at 587 nm, Förster distance R_0 ~6.3 nm. (C) Representative, deconvoluted 565 nm QD PL spectra following assembly with increasing mCherry. Inset, corresponding sensitized mCherry emission. (D) Plot of FRET efficiency vs mCherry-QD ratio corrected for heterogeneity[9c] and mCherry sensitization.

in sensing caspase 3 proteolysis.[8a,b] However, the mCherry utilized was expressed in *E. coli* and DHLA-capped QDs are incompatible with the slightly acidic cytoplasm as they require a basic pH to remain charged and dispersed. For expressing His_n-mCherry in eukaryotic cells, a two-step, site-directed mutagenesis was used to insert an N-terminal His_6 sequence into the eukaryotic pmCherry N1 expression plasmid (Clontech), detailed in the Supporting Information (S.I.). To be useful for *in vivo* assembly, QDs require both intracellular pH stability and the ability to still coordinate His_n-proteins. We surveyed four different PEGylated-QD preparations *in vitro* for these capabilities. The first two were eFluor 525 carboxylated QDs (eBioscience) and our 550 nm QDs solubilized with DSPE-PEG(2000) carboxylic acid-PEG lipid (Avanti Polar Lipids). These were meant to substitute for the EviTag lipid encapsulated QDs utilized by Dennis as they are no longer available.[7e] Working with *E. coli* derived mCherry-His_6,[8a] we found no evidence of self-assembly to these QDs even in the presence of added Ni^{2+} as probed by both gel electrophoresis and FRET (S.I.). Similar evaluation of our 550 nm QDs displaying a mixed 1:1 surface ratio of DHLA-PEG ligands terminating in carboxy:methoxy groups[8c] also did not evince any mCherry-His_6 coordination even with added Ni^{2+} (S.I.). Lastly, we tested Invitrogen Qdot 565 nm ITK carboxyl QDs. The electropherograms in Figure 2A clearly demonstrate mCherry-His_6 coordinating to these QDs and altering their mobility in the presence of 250 μM Ni^{2+}. At valences of 2−4 mCherry/QD, discrete bands corresponding to lower ratios of ~0, 1, and 2 proteins/QD are clearly visible. Gel mobility shifts plateau at ~16−20 mCherry/QD reflecting limited resolution rather than maximum loading. Assuming a 12.5 nm minimal diameter for these QDs (area ~490 nm^2) and a mCherry-QD interaction cross section of 5.5 nm^2 predicts ~90 mCherry could be maximally attached to these QDs.[9a,b] Viewing gel-separated QD conjugates at >625 nm to isolate mCherry emission while exciting the QDs at 365 nm showed a mCherry FRET-sensitization which increased with higher protein/QD valence. Indeed, at 20 mCherry/QD the sensitized emission is ≥3× that of equal control mCherry alone separated in the lane next to it. Figure 2C shows deconvoluted PL spectra from 565 nm ITK/Ni^{2+} QDs (250 μM Ni^{2+}) assembled with increasing mCherry-His_6 ratios along with the sensitized mCherry component. Similar to Rao's report,[7f] added Ni^{2+} increases QD-His_6 interactions and FRET (compare to without Ni^{2+}; Supporting Figure 3). Figure 2D plots the corresponding FRET efficiency and mCherry sensitization. Analysis derived a QD-core

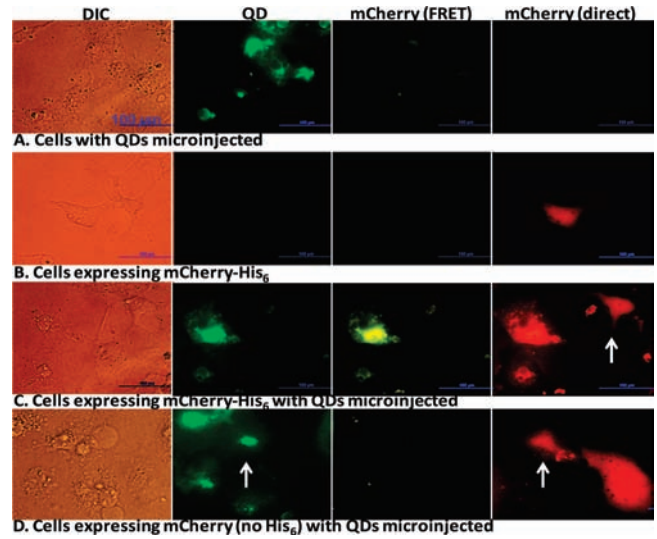

Figure 3. (A) COS-1 cells microinjected with 565 nm ITK/Ni^{2+} QDs. (B) Cell expressing mCherry-His_6 with no QDs present. (C) Cells expressing mCherry-His_6 microinjected with 565 nm ITK/Ni^{2+} QDs. Arrow indicates mCherry expressing cell without microinjected QDs. Note the lack of FRET signal from this cell. (D) Cells expressing control mCherry lacking His_6 and microinjected with 565 nm ITK/Ni^{2+} QDs. No FRET signal is evident. Arrow indicates cell expressing mCherry and injected with QDs.

to mCherry-chromophore separation distance r of ~11.3 nm, a value consistent with QD size if the 35 residue N-terminal linker present on this bacterial mCherry allele is in a fully extended conformation.[8] We surmise that, akin to Rao's interpretation,[7f] ITK QD-Ni^{2+} chelation allows mCherry-His_6 coordination analogous to NTA interactions, while the other QD ligands do not or sterically prevent direct Zn surface coordination.[6b,7]

Confident in the mCherry-His_6 ability to coordinate to 565 nm ITK carboxyl/Ni^{2+} QDs, we proceeded to evaluate intracellular assembly kinetics. Plasmid pmCherry-His_6 N1 was transfected into COS-1 cells resulting in ~40% of cells expressing fluorescent mCherry after 1 day. Adherent cells were microinjected with 2 μM 565 nm ITK QDs pretreated with/without 250 μM Ni^{2+}. Cell culture/transfection, QD preparation, microinjection, and imaging are detailed in the S.I. Figure 3 shows representative micrographs collected from the configurations tested. Panel A displays nontransformed cells injected with 565 nm ITK/Ni^{2+} QDs, while panel B shows a cell expressing mCherry-His_6 without QDs present. Negligible spectral leakage is seen in the mCherry-FRET channel (QD excitation with mCherry emission) or between channels. In panel C, cells expressing mCherry-His_6 were injected with 565 nm ITK/Ni^{2+} QDs and a sensitized mCherry emission overlapping both QD and mCherry direct fluorescence now appears in the FRET channel. More importantly, no FRET emission is seen from a cell expressing mCherry but not injected with QDs (white arrow). In panel D, cells expressing mCherry lacking the His_6 sequence did not produce any FRET emission when injected with the same QDs. Additional control experiments where 580 nm QDs functionalized with DHLA-PEG 1:1 carboxy:methoxy ligands with Ni^{2+} were microinjected into mCherry-His_6 expressing cells also did not result in FRET despite better spectral overlap (S.I.). Cumulatively, these data clearly confirm that 565 nm ITK/Ni^{2+} QD microinjection can allow cytoplasmic mCherry-His_6 to specifically assemble onto the QDs *in vivo*. Proximity-dependent FRET emission is only seen when His_6 coordinates the mCherry-acceptor to the QD-donor. The low mCherry sensitization initially noted with the bacterially expressed protein was partially mitigated in two ways. First, the COS-1 mCherry-His_6 was expressed with an ~80% shorter N-terminal linker (10 vs 35 residues) bringing the coordinated protein closer to the QD and improving FRET efficiency. Second, slightly longer exposure times collected more fluorescence from the sensitized FRET channel as needed.

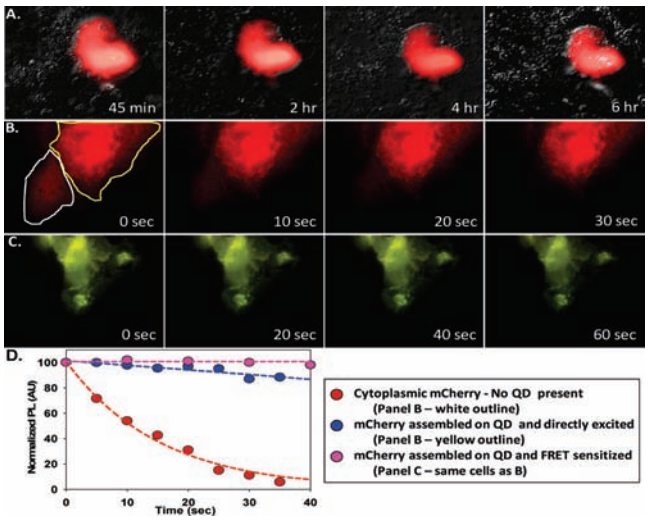

Figure 4. (A) COS-1 cell expressing mCherry-His_6 microinjected with 565 nm ITK/Ni^{2+} QDs and tracked for 6 h. (B) Direct mCherry excitation (λ_{ex} ~560 nm, λ_{em} ~630 nm) of side-by-side mCherry-expressing cells with/without QD over 30 s. Note photobleaching of non-QD injected cell (white outline) vs QD injected cell (yellow). (C) FRET excitation (λ_{ex} ~420 nm, λ_{em} ~630 nm) of cells in B for another 60 s. (D) Normalized, PL vs time from QD negative cell in B (red), QD-injected cell in B (blue), and QD FRET-sensitized mCherry emission from panel C (pink).

To monitor *in vivo* QD-mCherry conjugate stability over time and probe effects on cellular integrity, FRET-sensitized mCherry emission in QD-injected cells was tracked for 6 h following microinjection (Figure 4A, Supporting Figure 9). No loss of sensitized PL or changes in cellular morphology were observed suggesting that cellular processes could be investigated with the conjugates during this experimental time window. Lastly, we compared intracellular mCherry-His_6 PL during (1) cytoplasmic dispersion, (2) coordination to QDs, and (3) direct excitation or (4) sensitization by QDs. Side-by-side cells expressing mCherry-His_6 where only one had been microinjected with the QDs were probed. As seen in Figure 4B,D, we found that cytosolic mCherry rapidly photobleaches when directly excited, while QD-coordinated mCherry is unexpectedly far more photostable (90% vs 10% PL loss over 30 s, respectively). We subsequently switched illumination to the FRET mode and found the sensitized mCherry emission from these same cells to remain essentially unchanged over the next few minutes even following previous direct excitation (panels C,D). Results were confirmed by microinjecting cells from several different cultures (data not shown). Unexpectedly, QD-coordination appears to improve mCherry's photobleaching resistance. We speculate this may result from weaker direct irradiation of the coordinated/sensitized protein or changes in the attached protein's localized environment as QD coordination can allosterically alter mCherry conformation/rotation while PEG ligand interactions may change polarity or solvation.[10] Such processes have been suggested for the enhanced emission observed from organic dyes after labeling to antibodies.[10a] More pertinently, Niemeyer reported 75% increases in yellow fluorescent protein emission following attachment to oligonucleotides.[10b] In agreement, we note QD-coordinated mCherry-His_6 manifests a longer sensitized excited-state lifetime as compared to a directly excited free protein.[9a]

To date, *in vivo* QD labeling has predominantly targeted either accessible cell surface receptors[5,7c] or endosomal vesicles.[6] Here, we report a strategy for specifically labeling intracellular proteins with QDs *in vivo*. Using mCherry as a "model" target protein allows us to exploit its intrinsic fluorescence in combination with nanoscale FRET distance dependence to confirm intracellular QD assembly. We found improvements in the QD-attached mCherry photostability suggesting unanticipated optical benefits may be available to engineered QD-fluorescent protein sensors. The current strategy targets the His_6-affinity handle which is perhaps the most common modification introduced into proteins.[3c] Similar to intracellular labeling strategies with enzyme fusions that bind fluorescent substrates, the target protein here can be recombinantly expressed *in situ* in a "ready-to-conjugate" state and only requires the exogenous addition of a label, namely microinjection of QDs. However, in contrast to chimeric approaches, the small His_6 size significantly decreases the possibility of losing native protein function. Further, the resulting nanoarchitecture with multiple proteins centro-symmetrically arrayed around a central QD scaffold/donor can improve both FRET and binding avidity.[5d,6b] This chemistry expands the current intracellular labeling "toolset" and may allow many cytoplasmically expressed His_n-appended proteins to be labeled with QDs *in vivo*. Current interest in developing compact QDs while maintaining their ability to engage in metal-affinity coordination[7g] can complement this approach by bringing the proteins closer to the QDs for better FRET while simultaneously decreasing the overall conjugate size.

Acknowledgment. The authors acknowledge DTRA and NRL-NSI. K.B. and M.H.S. acknowledge ASEE and NRC fellowships.

Supporting Information Available: QD ligand structures, mCherry mutagenesis, gel electrophoresis, cell culture, transfection, microinjection, imaging, along with selected control data. Complete refs 2a, 5c, and 7g. This material is available free of charge via the Internet at http://pubs.acs.org.

References

(1) (a) Shaner, N. C.; Steinbach, P. A.; Tsien, R. Y. *Nat. Methods* **2005**, *2*, 905–909. (b) Giepmans, B. N. G.; Adams, S. R.; Ellisman, M. H.; Tsien, R. Y. *Science* **2006**, *312*, 217–224.

(2) (a) Los, G. V.; et al. *ACS Chem. Biol.* **2008**, *3*, 373–382. (b) Berrade, L.; Camarero, J. A. *Cell. Mol. Life Sci.* **2009**, *66*, 3909–3922. (c) George, N.; Pick, H.; Vogel, H.; Johnsson, N.; Johnsson, K. *J. Am. Chem. Soc.* **2004**, *126*, 8896–8897.

(3) (a) Adams, S. R.; Tsien, R. Y. *Nat. Protoc.* **2008**, *3*, 1527–1534. (b) Soh, N. *Sensors* **2008**, *8*, 1004–1024. (c) Hochuli, E.; Bannwarth, W.; Dobeli, H.; Gentz, R.; Stuber, D. *Bio/Technology* **1988**, *6*, 1321–1325.

(4) (a) Resch-Genger, U.; Grabolle, M.; Cavaliere-Jaricot, S.; Nitschke, R.; Nann, T. *Nat. Methods* **2008**, *5*, 763–775. (b) Tsien, R. Y. *Annu. Rev. Biochem.* **1998**, *67*, 509–544.

(5) (a) Michalet, X.; Pinaud, F. F.; Bentolila, L. A.; Tsay, J. M.; Doose, S.; Li, J. J.; Sundaresan, G.; Wu, A. M.; Gambhir, S. S.; Weiss, S. *Science* **2005**, *307*, 538–544. (b) Klostranec, J. M.; Chan, W. C. W. *Adv. Mater.* **2006**, *18*, 1953–1964. (c) Dif, A.; et al. *J. Am. Chem. Soc.* **2009**, *131*, 14738–14746. (d) Medintz, I. L.; Mattoussi, H. *Phys. Chem. Chem. Phys.* **2009**, *11*, 17–45.

(6) (a) Delehanty, J. B.; Mattoussi, H.; Medintz, I. L. *Anal. Bioanal. Chem.* **2009**, *393*, 1091–1105. (b) Delehanty, J. B.; Boeneman, K.; Bradburne, C. E.; Robertson, K.; Medintz, I. L. *Exp. Opin. Drug Delivery* **2009**, *6*, 1091–1112.

(7) (a) Sapsford, K. E.; Pons, T.; Medintz, I. L.; Higashiya, S.; Brunel, F. M.; Dawson, P. E.; Mattoussi, H. *J. Phys. Chem. C* **2007**, *111*, 11528–11538. (b) Medintz, I. L.; Konnert, J. H.; Clapp, A. R.; Stanish, I.; Twigg, M. E.; Mattoussi, H.; Mauro, J. M.; Deschamps, J. R. *Proc. Natl. Acad. Sci. U.S.A.* **2004**, *101*, 9612–9617. (c) Liu, W.; Howarth, M.; Greytak, A. B.; Zheng, Y.; Nocera, D. G.; Ting, A. Y.; Bawendi, M. G. *J. Am. Chem. Soc.* **2008**, *130*, 1274–1284. (d) Roullier, V.; Clarke, S.; You, C.; Pinaud, F.; Gouzer, G.; Schaible, D.; Marchi-Artzner, V.; Piehler, J.; Dahan, M. *Nano Lett.* **2009**, *9*, 1228–1234. (e) Dennis, A. M.; Bao, G. *Nano Lett.* **2008**, *8*, 1439–1445. (f) Yao, H.; Zhang, Y.; Xiao, F.; Xia, Z.; Rao, J. *Angew. Chem., Int. Ed.* **2007**, *46*, 4346–4349. (g) Liu, W.; et al. *J. Am. Chem. Soc.* **2010**, *132*, 472–483.

(8) (a) Medintz, I. L.; Pons, T.; Susumu, K.; Boeneman, K.; Dennis, A. M.; Farrell, D.; Deschamps, J. R.; Melinger, J. S.; Bao, G.; Mattoussi, H. *J. Phys. Chem. C* **2009**, *113*, 18552–18561. (b) Boeneman, K.; Mei, B. C.; Dennis, A. M.; Bao, G.; Deschamps, J. R.; Mattoussi, H.; Medintz, I. L. *J. Am. Chem. Soc.* **2009**, *131*, 3828–2829. (c) Mei, B. C.; Susumu, K.; Medintz, I. L.; Mattoussi, H. *Nat. Protoc.* **2009**, *4*, 412–423.

(9) (a) Prasuhn, D. E.; Deschamps, J. R.; Susumu, K.; Stewart, M. H.; Boeneman, K.; Blanco-Canosa, J. B.; Dawson, P. E.; Medintz, I. L. *Small* **2010**, *6*, 555–564. (b) Pons, T.; Uyeda, H. T.; Medintz, I. L.; Mattoussi, H. *J. Phys. Chem. B* **2006**, *110*, 20308–20316. (c) Pons, T.; Medintz, I. L.; Wang, X.; English, D. S.; Mattoussi, H. *J. Am. Chem. Soc.* **2006**, *128*, 15324–15331.

(10) (a) Gruber, H. J.; Hahn, C. D.; Kada, G.; Riener, C. K.; Harms, G. S.; Ahrer, W.; Dax, T. G.; Knaus, H. G. *Bioconjugate Chem.* **2000**, *11*, 696–704. (b) Kukolka, K.; Niemeyer, C. M. *Org. Biomol. Chem.* **2004**, *2*, 2203–2206.

JA100201W